# Samaria-Doped Ceria Electrolyte Supported Direct Carbon Fuel Cell with Molten Antimony as the Anode

**ARTICLE** *in* INDUSTRIAL & ENGINEERING CHEMISTRY RESEARCH · DECEMBER 2013

Impact Factor: 2.59 · DOI: 10.1021/ie403164c



**3 AUTHORS**, INCLUDING:

Xiaoyong Xu
University of Queensland
**110** PUBLICATIONS **937** CITATIONS

SEE PROFILE

Wei Zhou
Nanjing Tech University
**104** PUBLICATIONS **2,438** CITATIONS

SEE PROFILE

I&EC research
Industrial & Engineering Chemistry Research

Article

pubs.acs.org/IECR

# Samaria-Doped Ceria Electrolyte Supported Direct Carbon Fuel Cell with Molten Antimony as the Anode

Xiaoyong Xu, Wei Zhou,* and Zhonghua Zhu*

School of Chemical Engineering, The University of Queensland, St. Lucia, Queensland 4072, Australia

**ABSTRACT:** Direct carbon fuel cells can efficiently convert solid carbon fuel to electricity with an almost pure $CO_2$ exhaust stream, which can be readily collected for industry use or $CO_2$ sequestration, and thus could have a major impact on reducing fuel consumption and $CO_2$ emissions. Here, we report a high-performance samaria-doped ceria (SDC) electrolyte supported direct carbon fuel cell based upon a solid oxide fuel cell with a molten antimony anode. The area specific resistances associated with the molten Sb−$Sb_2O_3$ electrode are only 0.026, 0.045, and 0.121 Ω $cm^2$ at 750, 700, and 650 °C, respectively, while the maximum power outputs can reach 327, 268, and 222 mW $cm^{-2}$ at the corresponding temperatures. Moreover, SDC electrolyte shows the tolerance to corrosion of molten antimony at high temperature in the period investigated.

## 1. INTRODUCTION

Because of the world's growing energy demands, pollution concerns, and reliance upon limited fossil fuels, there has recently been significant interest in the development of fuel cells that can convert the chemical energy of carbon or biomass directly into electricity without a reforming process. Direct carbon fuel cells (DCFCs) are the most efficient and environmentally friendly technology to convert solid carbon energy to electricity without combustion or gasification. The thermodynamic efficiency of the DCFC can reach up to 100%, and the produced off-gas in the anode compartment is almost pure $CO_2$, which can be easily collected for industrial use or sequestration. Therefore, it could have a major impact on reducing fuel consumption and $CO_2$ emissions. There have been different attempts to convert carbon materials directly into electricity in the DCFC. According to the different electrolytes, DCFCs can be mainly grouped into three types, i.e., molten hydroxide,[1−5] molten carbonate,[6−12] and solid oxide electrolyte fuel cells.[13−25] Recently, lots of research has been carried out on DCFCs using solid oxide electrolytes (based upon solid oxide fuel cells, SOFCs) to separate the cathode and anode because advanced cathode materials can be used in these structured DCFCs. However, utilization of solid carbon fuels directly inside these fuel cells still presents serious challenges largely because of the difficulty in making physical contact between the fuel particles and charge-transfer reaction sites at the anode/electrolyte interface.[26−30] Various approaches were employed to improve the anode performance of the DCFC by adding different intermediaries into the anode chamber, including dispersing solid carbon in molten carbonate[13−18,20,21,31,32] or molten metal[22−25,33,34] in the anode compartment. Although molten carbonates exhibit high ionic conductivity at elevated temperature, they are poor electrical conductors that limit the performance of these cells. One of the most promising methods employs molten metal as the anode electrode, which not only has certain oxygen conductivity but also has high electrical conductivity.

Yentekakis et al.[35] designed the fuel cell with a molten iron bath as the anode in 1989. In this fused metal/yttria-stabilized zirconia (YSZ)/platinum, $O_2$ design, the fine carbon is fed to the fused iron anode as the fuel and air is fed into the cell's cathodic compartment. The design shows promising performance; however, it brings lots of challenges because the fuel cell must be operated over the melting point of iron (the melting point of iron is 1536 °C). CellTech Power LLC (CellTech) developed a layer of molten liquid tin as the anode to directly convert carbonaceous fuels including coal into electricity without gasification[36,37] at 800−1000 °C. Unfortunately, a solid $SnO_2$ layer formed at the electrolyte interface was observed during fuel-cell operation at 700 °C, and it inhibits further transfer of the oxygen from the tin/electrolyte interface, resulting in high anode losses.[22] Therefore, it is crucial to develop the fuel cell with a molten bath, and both the metal and metal oxide should have a low melting point. Later, Jayakumar et al.[24] examined indium (In), lead (Pb), antimony (Sb), bismuth (Bi), and silver (Ag) as anodes. The electrode resistance associated with molten antimony is only approximately 0.06 Ω $cm^2$ so that a peak power density of 350 mW $cm^{-2}$ at 700 °C is obtained, although the calculated open circuit voltage (OCV) for the Sb−$Sb_2O_3$ mixture is only 0.75 V. However, the mechanisms of the electrochemical reactions and redox and transport processes within the liquid metal electrodes are still unclear. With scandium-stabilized zirconia used as the electrolyte in these studies, severe corrosion of the electrolyte in molten antimony occurred in regions of high current flow, while no corrosion was observed with YSZ as the electrolyte operating at the same current densities.[39] However, the ionic conductivities of YSZ are 1 order of magnitude lower than those of scandium-stabilized zirconia. The ionic conductivities of samaria-doped ceria (SDC) are comparable to those of scandium-stabilized zirconia. On the basis of the research by Jayakumar et al.,[24] we have investigated an SDC-electrolyte-supported DCFC with a molten antimony anode in this paper. Thermodynamic analysis is discussed in this study. Good

**Received:** September 23, 2013
**Revised:** November 25, 2013
**Accepted:** November 27, 2013
**Published:** November 27, 2013

  

performance can be achieved by operating on activated carbon fuels, even at 650 °C.

## 2. EXPERIMENTAL SECTION

The aim of the present study is to study the anode performance. Therefore, it is crucial to choose the advanced cathode and electrolyte materials with a small amount of resistance in order to operate the fuel cell with a sensitive anode performance. Therefore, the cathode $Ba_{0.5}Sr_{0.5}Co_{0.8}Fe_{0.2}O_{3-\delta}$ (BSCF) was used in the present study because the area specific resistance (ASR) of the BSCF cathode is only ~0.05 Ω $cm^2$ at 650 °C.[38]

The SDC electrolyte pellets with thickness of ~200 μm and diameter of 14 mm were prepared by dry pressing commercial SDC powder (NexTech) and sintering at 1400 °C for 5 h. BSCF powders, synthesized by a combined ethylenediaminetetraacetic acid–citrate complexing process, were mixed with 2-propanol and glycerol using a ball mill for 2 h to form BSCF ink. The BSCF ink was sprayed onto the other side of the SDC pellet as the cathode. The sintering temperature of the cathode was 1000 °C, and the geometric surface area of the cathode was 0.28 $cm^2$. Silver paste was painted on the cathode side as the current collector. Next, 2 g of antimony powder (100 mesh, 99.5%, ALFA) was poured into the alumina tube to form the molten anode, 0.5 g of activated carbon was placed on top of it, and then pure nitrogen gas was purged into the anode compartment as a protection gas. The fuel cell was tested in a top-loading furnace. Rhenium wires were inserted into the molten antimony bath and used for current collection on the anode side. The structure of the fuel cell employed in this study is similar to the previous designs, as described in refs 23 and 24. The schematic of the setup is shown in Figure 1.

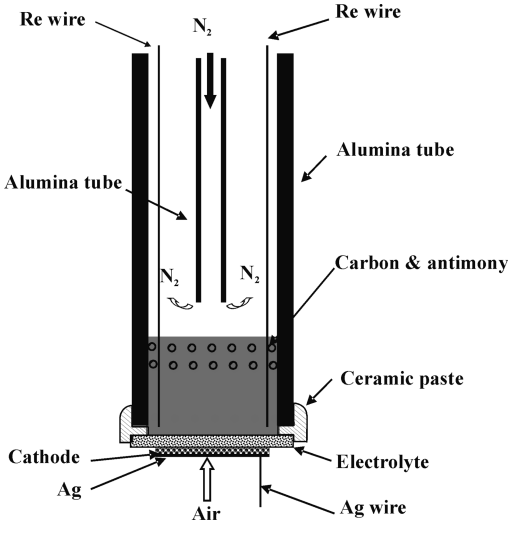


**Figure 1.** Schematic of the experimental setup.

Electrochemical measurements were carried out using an Autolab PGSTAT30 electrochemical workstation with the GPES and FRA software package (version 4.9). *I*–*V* curves were measured by a potential sweep at a scan rate of 0.1–5 V $s^{-1}$ once a steady OCV was reached. The tests were repeated several times until a stable performance was achieved. Electrochemical impedance spectroscopy spectra of the fuel cell were also obtained on an Autolab PGSTAT30 electrochemical workstation with a frequency range from 100 kHz to 0.01 Hz and a signal amplitude of 10 mV under OCV conditions.

## 3. RESULTS AND DISCUSSION

**3.1. OCVs at Different Temperatures.** The ideal potential for the liquid antimony anode can be expressed the same as any other fuel cell.[37] It can be written as

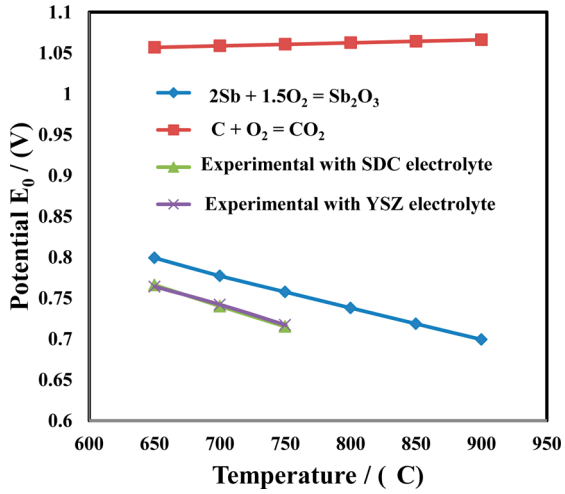


**Figure 2.** Theoretical standard potentials based on two reactions (2Sb + $1.5O_2$ = $Sb_2O_3$ and C + $O_2$ = $CO_2$) and measured OCVs.

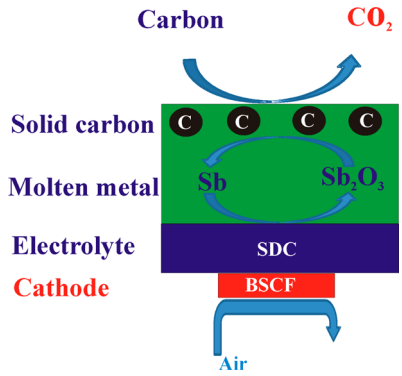


**Figure 3.** DCFC with a molten antimony anode.

$$E_{cell} = -\Delta G^{\circ}/nF + RT\ \ln(a_{Sb_2O_3}/a_{Sb}^{2}a_{O_2}^{1.5})/nF \quad (1)$$

where $\Delta G^{\circ}$ is the reaction Gibbs function, $n$ is the number of electrons in the electrochemical reaction (here $n$ = 6), and $a_{Sb_2O_3}$, $a_{Sb}$, and $a_{O_2}$ are the activities of $Sb_2O_3$, Sb at the anode, and $O_2$ at the cathode, respectively. Both $a_{Sb_2O_3}$ and $a_{Sb}$ are 1 because $Sb_2O_3$ is a pure oxide phase and Sb is a pure metal phase, and $a_{O_2}$ is 0.21 because air is employed in the cathode compartment.

Figure 2 shows the calculated Nernst potential plotted over a range of temperatures based on two reactions (2Sb + $1.5O_2$ = $Sb_2O_3$ and C + $O_2$ = $CO_2$) using thermodynamic calculation software *FACTSAGE*[39] and the OCV measured in this study. The measurement went from high to low temperature. Theoretical standard OCVs of these listed reactions, shown in this figure, are calculated based on an activity of 1 for all reactants, except the activity of 0.21 for oxygen in air. The measured OCVs at the temperature range investigated in the


dx.doi.org/10.1021/ie403164c | Ind. Eng. Chem. Res. 2013, 52, 17927–17933

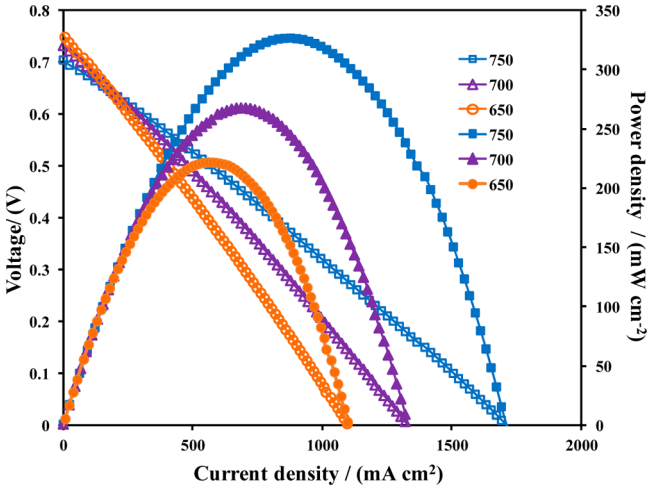


**Figure 4.** *V*–*I* polarization and power density curves for the DCFC with the molten antimony anode at 650, 700, and 750 °C.

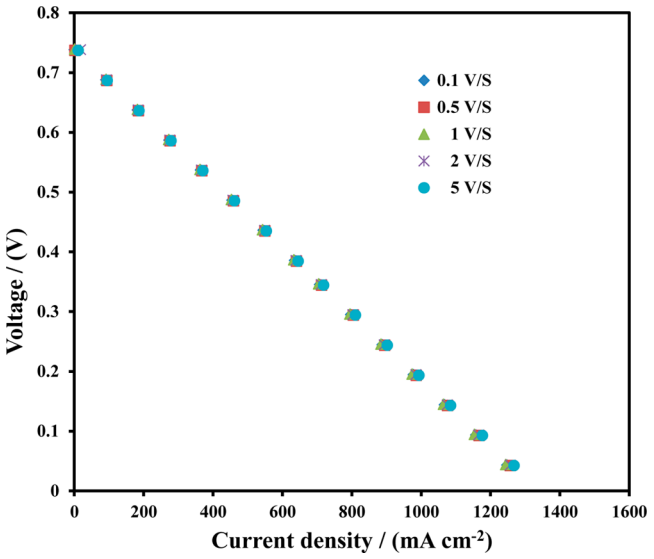


**Figure 5.** Effect of the scan rate on *V*–*I* polarization for the DCFC with the molten antimony anode at 700 °C.

present study were a little lower than the calculated theoretical standard OCVs for a molten-antimony-based SOFC and decreased slightly with increasing temperature, indicating that the OCVs are governed by the reaction $2Sb + 1.5O_2 = Sb_2O_3$. SDC or gadolinia-doped ceria electrolyte used in a SOFC leads to a lower OCV compared to the YSZ electrolyte because of partial reduction of $Ce^{4+}$ in highly reducing atmospheres such as $H_2$.[40] However, this is not the case when molten antimony is used in the anode, attributed to the lower reducibility of molten antimony. To identify whether the lower OCVs are the result of the critical drawback of the ceria electrolyte (its partial electronic conductivity at reduced conditions),[41] the OCVs with YSZ electrolytes were also measured and compared with the ones with SDC electrolytes at the temperature range investigated in the present study. The similar results shown in Figure 2 indicate that the lower OCVs are not due to the partial electronic conductivity of SDC but are possibly ascribed to the error from the calculated theoretical standard OCVs.

**3.2. Driving Force of Anode Reactions.** In the operation of this fuel cell, the molten antimony anode works as an

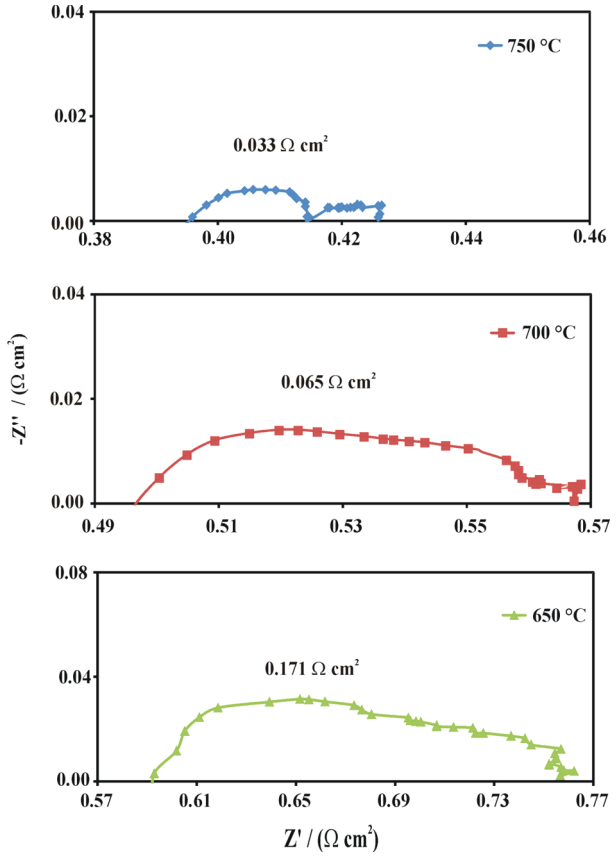


**Figure 6.** Impedance spectra for the DCFC with the molten antimony anode at 650, 700, and 750 °C.

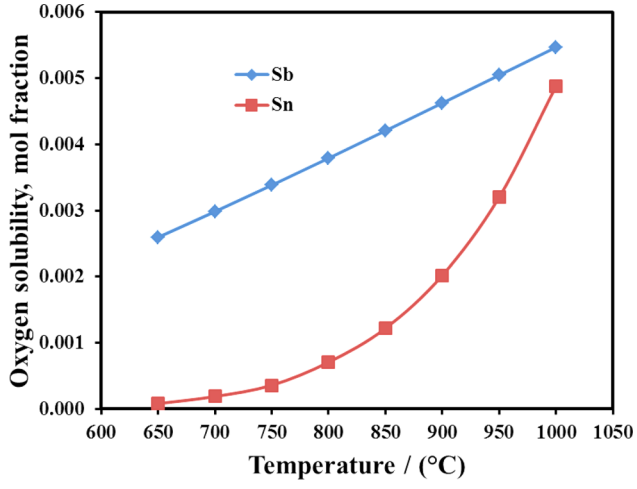


**Figure 7.** Maximum solubility of oxygen in molten antimony and tin.

intermediary to deliver oxygen ion to carbon fuel; the anode reaction can be described in the following two reactions.

$$2Sb + 3O^{2-} \leftrightarrow Sb_2O_3 + 6e^- \quad (2)$$

$$Sb_2O_3 + 1.5C \leftrightarrow 2Sb + 1.5CO_2 \quad (3)$$

As shown in Figure 3, the electrochemical reaction (2) occurs at the molten metal anode–electrolyte interface, where molten metal works not only as a fuel but also as an electrical conductor. The molten metal will be oxidized and delivered to oxidize the carbon fuel as an "intermediary". Metal oxide will be


dx.doi.org/10.1021/ie403164c | Ind. Eng. Chem. Res. 2013, 52, 17927–17933

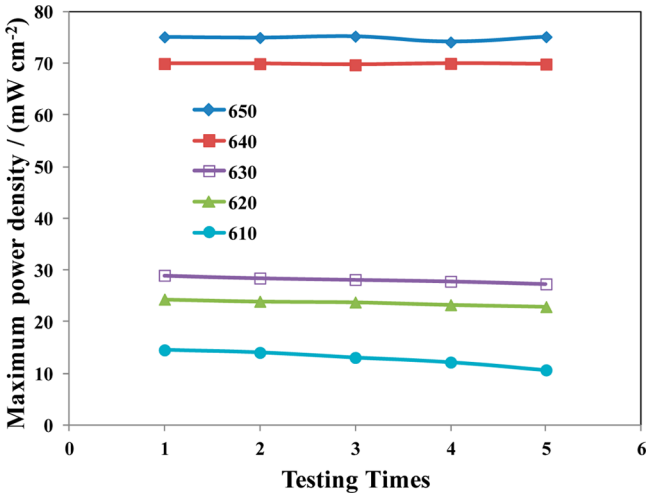


**Figure 8.** Measured maximum power densities with time between 610 and 650 °C.

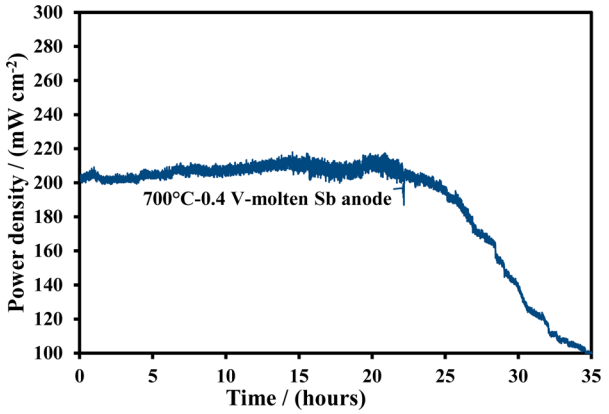


**Figure 9.** Stability of the DCFC with a molten antimony anode and activated carbon fuel at 700 °C.

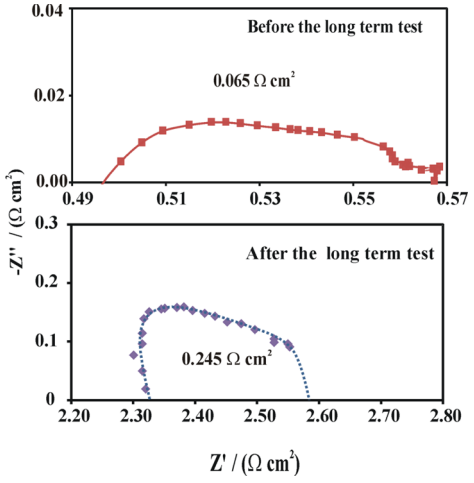


**Figure 10.** Impedance spectrum before and after the long-term test at 700 °C.

reduced to molten metal through reaction (3) at the carbon fuel–molten antimony interface. On basis of OCV analysis, the anode performance is controlled by reaction (2).

**3.3. Performance of a SDC-Supported DCFC with a Molten Antimony Anode.** Figure 4 shows the *I*–*V* and *I*–*P* curves of a SDC-supported SOFC with a BSCF cathode at various temperatures; molten antimony and some activated carbon were applied in the anode, and ambient air served as the cathode atmosphere during the measurement. The OCV reached 0.766, 0.741, and 0.715 V at 750, 700, and 650 °C, respectively, while the maximum power outputs reached 327, 268, and 222 mW $cm^{-2}$ at corresponding temperatures.

The *I*–*V* curves measured in this study are almost linear over the whole range of current densities obtained, implying that the cell impedance is nearly independent of the current density.[23] Furthermore, the *I*–*V* curves in Figure 5 obtained at different scan rates ranging from 0.1 to 5 V $s^{-1}$ are almost the same at the same temperature, indicating that the concentration polarization (mass-transfer or gas-diffusion polarization) resistance is negligible in the present study conditions.

Figure 6 shows the EIS spectrum of a single cell under open-circuit conditions for the resistance distribution of the cell with BSCF electrodes from polarization and electrolyte ohmic resistances. The total ASRs of the cell are 0.427, 0.561, and 0.763 Ω $cm^2$ at 750, 700, and 650 °C, respectively, consistent with the slope of the *I*–*V* curves in Figure 5, while the ohmic resistances of the cell are 0.394, 0.496, and 0.592 Ω $cm^2$ at 750, 700, and 650 °C, respectively. The ionic conductivities of the SDC electrolyte are calculated to be 0.051, 0.040, and 0.034 S $cm^{-1}$ at corresponding temperatures, respectively, and they are comparable to the data supplied by NextTech. Approximately 90% of the cell resistance is due to the 200 μm SDC electrolyte. Given that the losses associated with an identical BSCF cathode have been reported to be approximately 0.007, 0.020, and 0.050 Ω $cm^2$ at 750, 700, and 650 °C,[38] respectively, the losses associated with the molten Sb–$Sb_2O_3$ electrode are only 0.026, 0.045, and 0.121 Ω $cm^2$ at corresponding temperatures. The value at 700 °C is close to the data (0.06 Ω $cm^2$) reported by Jayakuma et al.[23,24]

The molten antimony anode acts as an intermediary for oxygen transfer between the electrolyte and fuel. The oxygen solubility in antimony is thus a significant operating parameter because the effective oxygen conductivity in the molten antimony anode is directly proportional to the oxygen concentration. The solubility of oxygen in molten tin and antimony has been widely investigated. The maximum solubility of oxygen in molten tin and antimony was calculated based on the data from Belford and Alcock[42] and Heshmatpour and Stevenson[43] in Figure 7. Also, the maximum solubility of oxygen in molten tin and antimony increases with temperatures of 650 and 1000 °C. It is much higher in molten antimony than in molten tin, especially at low temperature. This could be one of the reasons why molten antimony is better than molten tin as the anode.

**3.4. Stability of a DCFC with a Molten Antimony Anode.** It is suggested that reducing the operating temperature of the DCFCs has a lot of benefits, such as rapid start-up and cool-down cycles as well as less expensive materials for cell fabrication. The reported melting points of antimony and antimony oxide are only 631 and 656 °C, respectively.[44] In order to investigate the stability of the antimony anode at low temperature (below 650 °C), the *I*–*V* performances have been repeatedly tested five times in the range of 610–650 °C. As shown in Figure 8, the measured maximum power densities are constant with time at 640 and 650 °C, while they decrease with time at lower temperatures (610–630 °C). Furthermore, the maximum power densities decrease with temperature, and they decrease drastically from 640 to 630 °C. It seems that once


dx.doi.org/10.1021/ie403164c | Ind. Eng. Chem. Res. 2013, 52, 17927–17933

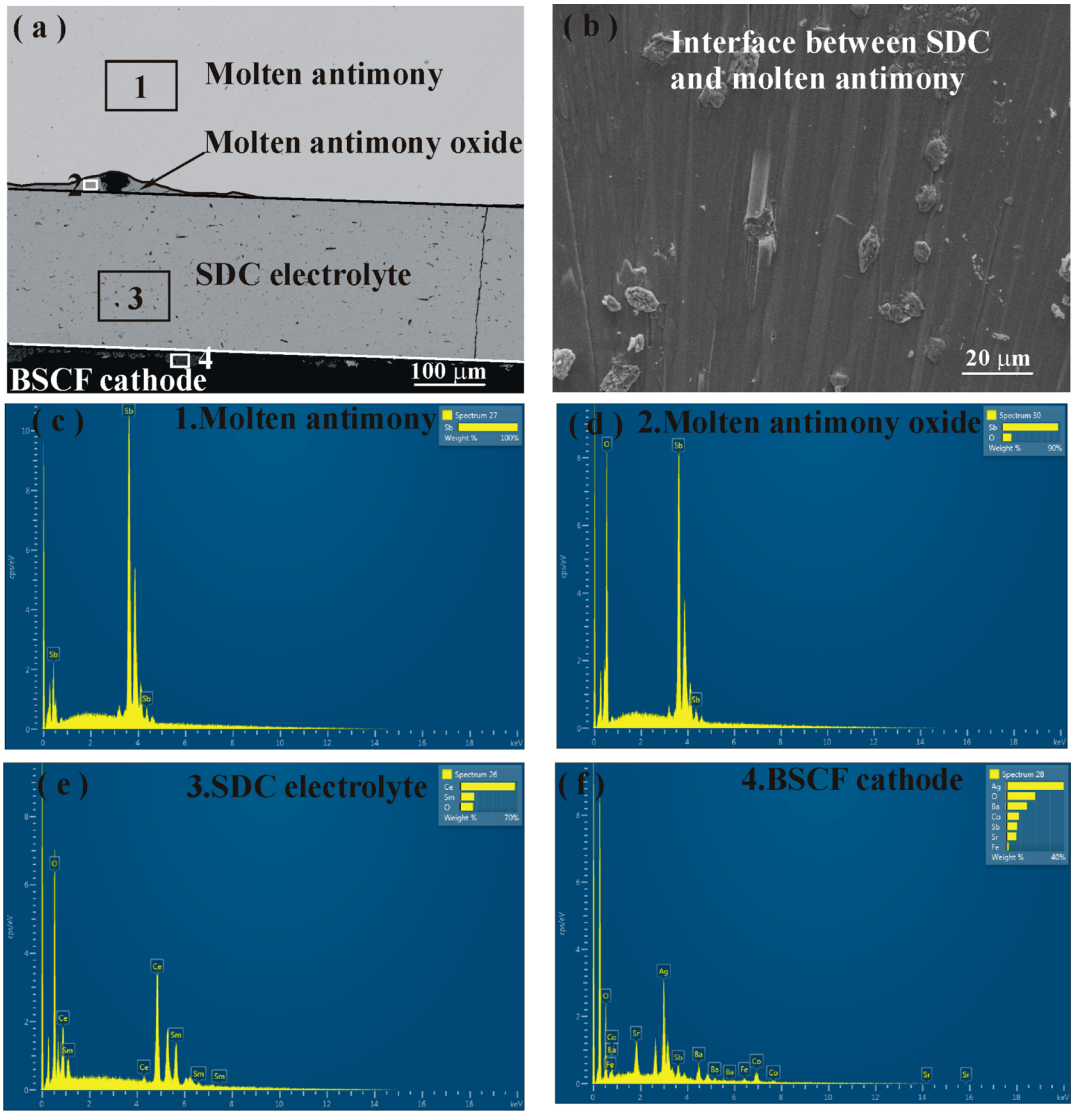


**Figure 11.** (a) Backscattered SEM micrographs of a section of fuel cell. (b) Interface between SDC and molten antimony. (c–f) EDX spectra from different sections of the fuel cell.

antimony becomes solid, the fuel cell performance deteriorates steadily with time, which is due to the lower oxygen diffusion rate in solid antimony relative to molten antimony.

The long-term stability of DCFCs is a problem in their practical applications.[31] We investigated the stability of the DCFC under 0.4 V at 700 °C. No stirring was used because the setup of the DCFC is very small in this study. Figure 9 shows the performance for a cell with 2 g of antimony and 0.5 g of activated carbon loaded on top of antimony. The monitored cell power density started to decrease from ~200 mW $cm^{-2}$ at 22 h operation with a degradation rate of 50% in 35 h. It is worth noting that the output of the power density vibrates in the range of 200–215 mW $cm^{-2}$. This vibration of the power density is likely due to the slow displacement of $Sb_2O_3$ by Sb, which could be improved by stirring.

The performance of the fuel cell with a molten antimony anode is stable in the first 22 h, showing a gradual decrease in the power density afterward. Exhaustion of the fuel could be one reason for such a performance degradation. To identify whether this point is the case, we calculated the theoretical working time of the fuel cell based on the amount of antimony and carbon fuel. The performance can last 9.2 h assuming that all antimony is consumed under the given current density of 512.5 mA $cm^{-2}$ with an electrode area of 0.28 $cm^2$, while it can last 31.1 h if 0.5 g of carbon is oxidized to $CO_2$.[24] In total, the fuel cell should last more than 40 h until the antimony and carbon are used up. However, the performance starts to decrease after 22 h, which is probably due to the slow displacement of $Sb_2O_3$ by Sb without stirring; some antimony oxide was formed and observed in the interface between the SDC electrolyte and molten antimony metal (Figure 11a,b). On the other side, the impedance spectra tested under OCV before and after the long-term test were collected and compared, and energy-dispersive X-ray (EDX) spectra were also collected from the section of the fuel cell. The corresponding impedance spectra tested under an open circuit are shown in Figure 10. Before the long-term test, the total ASR of the cell is at 0.561 Ω $cm^2$ and the ohmic resistance of the cell is 0.496 Ω $cm^2$. As shown in Figure 10, the impedance spectrum after the long-term test has a total ASR of 2.568 Ω $cm^2$ and the ohmic resistance increases to 2.320 Ω $cm^2$. Therefore, the decrease of the power densities in Figure 9 is


dx.doi.org/10.1021/ie403164c | Ind. Eng. Chem. Res. 2013, 52, 17927–17933

attributed to not only the increased ohmic resistance but also the worsened electrode performance. Figure 11a shows the backscattered scanning electron microscopy (SEM) micrographs of a section of the fuel cell, and parts c–f of Figure 11 show EDX spectra from different sections of the fuel cell. A layer of molten antimony oxide was formed at the interface between the SDC electrolyte and molten antimony (Figure 11b,d). It could be one of the reasons for the increased ohmic resistance, but this problem can be readily resolved by stirring the molten anode. As shown in Figure 11f, the BSCF cathode was found to be contaminated by antimony and was not in good contact with the SDC electrolyte, which can lead to increases in both the ohmic and cathode resistances. Interestingly, there is no evidence that molten antimony can corrode the SDC electrolyte in the period that we investigated considering that no antimony element was observed in the SDC electrolyte and no cerium and samarium elements were observed in molten antimony oxide. The antimony in the BSCF cathode was possibly due to the fragile property of the SDC electrolyte or poor sealing. We will carry out a comprehensive investigation on it hereafter.

## 4. CONCLUSIONS

We have investigated an SDC electrolyte-supported DCFC with a molten $Sb–Sb_2O_3$ anode. This molten $Sb–Sb_2O_3$ electrode enables facile oxygen transfer from the electrolyte to solid fuels at intermediate temperature. An ASR associated with the molten $Sb–Sb_2O_3$ electrode is comparatively small even at 650 °C. The present laboratory-scale system demonstrated high current densities with the feasibility of solid carbon direct conversion and $CO_2$ capture.

## AUTHOR INFORMATION


### Corresponding Authors

*Tel: +61-733653528. Fax +61-733654199. E-mail: wei.zhou@uq.edu.au.

*Tel: +61-733653528. Fax +61-733654199. E-mail: z.zhu@uq.edu.au.


### Notes

The authors declare no competing financial interest.

## ACKNOWLEDGMENTS

We acknowledge support of an Australian Research Council Linkage Project grant (LP100200002).

## REFERENCES


(1) Jacques, W. W. Method of converting the potential energy of carbon into electricity. U.S. Patent 555,511, Mar 3, 1896.

(2) Zecevic, S.; Patton, E. M.; Parharni, P. Carbon–air fuel cell without a reforming process. *Carbon* **2004**, *42*, 1983–1993.

(3) Hackett, G. A.; Zondlo, J. W.; Svensson, R. Evaluation of carbon materials for use in a direct carbon fuel cell. *J. Power Sources* **2007**, *168*, 111–118.

(4) Nunoura, T.; Dowaki, K.; Fushimi, C.; Allen, S.; Meszaros, E.; Antal, M. J. Performance of a First-Generation, Aqueous-Alkaline Biocarbon Fuel Cell. *Ind. Eng. Chem. Res.* **2007**, *46*, 734–744.

(5) Zecevic, S.; Patton, E. M.; Parhami, P. Direct electrochemical power generation from carbon in fuel cells with molten hydroxide electrolyte. *Chem. Eng. Commun.* **2005**, *192*, 1655–1670.

(6) Peelen, W. H. A.; Olivry, M.; Au, S. F.; Fehribach, J. D.; Hemmes, K. Electrochemical oxidation of carbon in a 62/38 mol % Li/K carbonate melt. *J. Appl. Electrochem.* **2000**, *30*, 1389–1395.

(7) Selman, J. R. Molten-salt fuel cells—Technical and economic challenges. *J. Power Sources* **2006**, *160*, 852–857.

(8) Steinberg, M. Conversion of fossil and biomass fuels to electric power and transportation fuels by high efficiency integrated plasma fuel cell (IPFC) energy cycle. *Int. J. Hydrogen Energy* **2006**, *31*, 405–411.

(9) Li, X.; Zhu, Z. H.; Chen, J. L.; De Marco, R.; Dicks, A.; Bradley, J.; Lu, G. Q. Surface modification of carbon fuels for direct carbon fuel cells. *J. Power Sources* **2009**, *186*, 1–9.

(10) Li, X.; Zhu, Z. H.; De Marco, R.; Bradley, J.; Dicks, A. Modification of Coal as a Fuel for the Direct Carbon Fuel Cell. *J. Phys. Chem. A* **2010**, *114*, 3855–3862.

(11) Li, X.; Zhu, Z.; Marcob, R. D.; Bradleya, J.; Dicksa, A. Evaluation of raw coals as fuels for direct carbon fuel cells. *J. Power Sources* **2010**, *195*, 4051–4058.

(12) Li, H. J.; Liu, Q. H.; Li, Y. D. A carbon in molten carbonate anode model for a direct carbon fuel cell. *Electrochim. Acta* **2010**, *55*, 1958–1965.

(13) Jain, S. L.; Lakeman, J. B.; Pointon, K. D.; Irvine, J. T. S. A novel direct carbon fuel cell concept. *J. Fuel Cell Sci. Technol.* **2007**, *4*, 280–282.

(14) Jain, S. L.; Nabae, Y.; Lakeman, B. J.; Pointon, K. D.; Irvine, J. T. S. Solid state electrochemistry of direct carbon/air fuel cells. *Solid State Ionics* **2008**, *179*, 1417–1421.

(15) Nabae, Y.; Pointonb, K. D.; Irvine, J. T. S. Electrochemical oxidation of solid carbon in hybrid DCFC with solid oxide and molten carbonate binary electrolyte. *Energy Environ. Sci.* **2008**, *1*, 148–155.

(16) Nabae, Y.; Pointon, K. D.; Irvine, J. T. S. Ni/C Slurries Based on Molten Carbonates as a Fuel for Hybrid Direct Carbon Fuel Cells. *J. Electrochem. Soc.* **2009**, *156*, B716–B720.

(17) Jiang, C.; Irvine, J. T. S. Short communication: Catalysis and oxidation of carbon in a hybrid direct carbon fuel cell. *J. Power Sources* **2011**, *196*, 7318–7322.

(18) Jiang, C.; Ma, J.; Bonaccorso, A. D.; Irvine, J. T. S. Demonstration of high power, direct conversion of waste-derived carbon in a hybrid direct carbon fuel cell. *Energy Environ. Sci.* **2012**, *5*, 6973–6980.

(19) Ju, H.; Uhm, S.; Kim, J. W.; Song, R. H.; Choi, H.; Lee, S. H.; Lee, J. Enhanced anode interface for electrochemical oxidation of solid fuel in direct carbon fuel cells: The role of liquid Sn in mixed state. *J. Power Sources* **2012**, *198*, 36–41.

(20) Jain, S. L.; Lakeman, J. B.; Pointon, K. D.; Marshall, R.; Irvine, J. T. S. Electrochemical performance of a hybrid direct carbon fuel cell powered by pyrolysed MDF. *Energy Environ. Sci.* **2009**, *2*, 687–693.

(21) Nurnberger, S.; Bussar, R.; Desclaux, P.; Franke, B.; Rzepka, M.; Stimming, U. Direct carbon conversion in a SOFC-system with a non-porous anode. *Energy Environ. Sci.* **2010**, *3*, 150–153.

(22) Jayakumar, A.; Lee, S.; Hornes, A.; Vohs, J. M.; Gorte, R. J. A Comparison of Molten Sn and Bi for Solid Oxide Fuel Cell Anodes. *J. Electrochem. Soc.* **2010**, *157*, B365–B369.

(23) Jayakumar, A.; Vohs, J. M.; Gorte, R. J. Molten-Metal Electrodes for Solid Oxide Fuel Cells. *Ind. Eng. Chem. Res.* **2010**, *49*, 10237–10241.

(24) Jayakumar, A.; Ungas, R. K.; Roy, S.; Javadekar, A.; Buttrey, D. J.; Vohs, J. M.; Gorte, R. J. A direct carbon fuel cell with a molten antimony anode. *Energy Environ. Sci.* **2011**, *4*, 4133–4137.

(25) Javadekar, A.; Jayakumar, A.; Pujara, R.; Vohs, J. M.; Gorte, R. J. Molten silver as a direct carbon fuel cell anode. *J. Power Sources* **2012**, *214*, 239–243.

(26) Cao, D. X.; Sun, Y.; Wang, G. L. Direct carbon fuel cell: Fundamentals and recent developments. *J. Power Sources* **2007**, *167*, 250–257.

(27) Desclaux, P.; Nurnberger, S.; Stimming, U. *Innovations in Fuel Cell Technologies*; Royal Society of Chemistry: London, 2010.

(28) Zhou, J.; Ye, X. F.; Shao, L.; Zhang, X. P.; Qian, J. Q.; Wang, S. R. *Electrochim. Acta* **2012**, *74*, 267–270.

(29) Jia, L. J.; Tian, Y.; Liu, Q. H.; Xia, C.; Yu, J. S.; Wang, Z. M.; Zhao, Y. C.; Li, Y. D. A direct carbon fuel cell with (molten carbonate)/(doped ceria) composite electrolyte. *J. Power Sources* **2010**, *195*, 5581–5586.

(30) Cantero-Tubilla, B.; Xu, C.; Zondlo, J. W.; Sabolsky, K.; Sabolsky, E. M. Investigation of anode configurations and fuel mixtures on the performance of direct carbon fuel cells (DCFCs). *J. Power Sources* **2013**, *238*, 227−235.
(31) Xu, X.; Zhou, W.; Liang, F.; Zhu, Z. Optimization of a direct carbon fuel cell for operation below 700 °C. *Int. J. Hydrogen Energy* **2013**, *38*, 5367−5374.
(32) Xu, X.; Zhou, W.; Liang, F.; Zhu, Z. A comparative study of different carbon fuels in an electrolyte-supported hybrid direct carbon fuel cell. *Appl. Energy* **2013**, *108*, 402−409.
(33) Jayakumara, A.; Javadekarb, A.; Küngasa, R.; Buttreyb, D. J.; Vohsa, J. M.; Gortea, R. J. Characteristics of Molten Metals as Anodes for Direct Carbon Solid Oxide Fuel Cells. *ECS Trans.* **2012**, *41*, 149−158.
(34) Jayakumar, A.; Javadekar, A.; Gissinger, J.; Vohs, J. M.; Huber, G. W.; Gorte, R. J. The stability of direct carbon fuel cells with molten Sb and Sb−Bi alloy anodes. *AIChE J.* **2013**, *59*, 3342−3348.
(35) Yentekakis, I. V.; Debenedetti, P. G.; Costa, B. A Novel Fused Metal Anode Solid Electrolyte Fuel-Cell for Direct Coal-Gasification—a Steady-State Model. *Ind. Eng. Chem. Res.* **1989**, *28*, 1414−1424.
(36) McPhee, W. A. G.; Bateman, L.; Koslowske, M.; Slaney, M.; Uzep, Z.; Bentley, J.; Tao, T. Direct JP-8 Conversion Using a Liquid Tin Anode Solid Oxide Fuel Cell (LTA-SOFC) for Military Applications. *J. Fuel Cell Sci. Technol.* **2011**, *8*, 041007.
(37) Abernathy, H.; Gemmen, R.; Gerdes, K.; Koslowske, M.; Tao, T. Basic properties of a liquid tin anode solid oxide fuel cell. *J. Power Sources* **2011**, *196*, 4564−4572.
(38) Shao, Z. P.; Haile, S. M. A high-performance cathode for the next generation of solid-oxide fuel cells. *Nature* **2004**, *431*, 170−173.
(39) www.factsage.com, Sept 7, 2013.
(40) Kulkarni, A.; Giddey, S.; Badwal, S. P. S. Electrochemical performance of ceria−gadolinia electrolyte based direct carbon fuel cells. *Solid State Ionics* **2011**, *194*, 46−52.
(41) Yoo, H. I.; Park, S. H.; Chun, J. Suppression of Electronic Conductivity of $CeO_2$-Based Electrolytes by Electron Traps. *J. Electrochem. Soc.* **2010**, *157*, B215−B219.
(42) Belford, T. N.; Alcock, C. B. Thermodynamics and solubility of oxygen in liquid metals from e.m.f. measurements involving solid electrolytes. Part 2. Tin. *Trans. Faraday Soc.* **1965**, *61*, 443−453.
(43) Heshmatpour, B.; Stevenson, D. A. An electrochemical study of the solubility and diffusivity of oxygen in the respective liquid metals indium, gallium, antimony and bismuth. *J. Electroanal. Chem. Interfacial Electrochem.* **1981**, *130*, 47−55.
(44) http://en.wikipedia.org/, Sept 7, 2013.